J Appl Electrochem (2010) 40:1853–1858
DOI 10.1007/s10800-010-0141-7

ORIGINAL PAPER

A mechanistic model of the gas film dynamics during the electrochemical discharge phenomenon

R. El-Haddad · R. Wüthrich

Received: 4 January 2010 / Accepted: 15 April 2010 / Published online: 18 May 2010

Abstract A model for the prediction of the current–voltage characteristics of a two electrodes cell incorporating the dynamics of the gas film formed during the electrochemical discharge phenomenon is developed. In its mean-field version, the model presents good qualitative agreement but overestimates the hysteresis effect and predicts too large current densities for the cell operation once the gas film is formed. An improved stochastic model, which assumes gas film departures from the electrode surface according to a Poisson process, addresses these issues and gives significantly better predictions. Two relations are presented which allow estimating the mean gas film detachment time and its variance from the experimental study of the hysteresis in the forward and reverse scan of a two electrode cell operated at high current densities.

Keywords Electrochemical discharge phenomenon · Hysteresis · Bistability · Anode/cathode effect · Gas film life-time

List of symbols

A	Electrode surface (m^2)
F	Faraday constant (C mol^{-1})
h_b	Effective average bubble height (m)
I	Current (A)
j^{crit}	Nominal critical current density, nominal current density at which a gas film can be formed (A m^{-2})
j_{local}	Local current density (A m^{-2})
N	Number of lattice sites per surface (m^{-2})
n	Stoichiometric number
n_s	Average normalised number (per total number of lattice sites) of clusters of size s
P	Average size of infinite cluster (in number of sites per total number of sites in the lattice)
p	Pressure (Pa)
p_c	Percolation threshold
R	Ideal gas constant (J K^{-1} mol^{-1})
$R(\theta)$	Inter-electrode resistance (with the presence of bubbles) (Ω)
R^{bulk}	Bulk inter-electrode resistance (without the presence of bubbles) (Ω)
s	Cluster size (in number of lattice sites)
T	Temperature (K)
t	Time (s)
t_f	Average gas film formation time (s)
U	Cell terminal voltage (V)
U^{crit}	Critical voltage, voltage at which a gas film can be formed (V)
U_d	Water decomposition potential (V)
V_b	Volume of a gas bubble of size $s = 1$ (m^3)
$\dot{V}_g$	Gas volume per unit of time (m^3 s^{-1})
v	Voltage scan rate (V s^{-1})
z	Charge number
β	Coefficient of Faradic gas production (m^3 s^{-1} A^{-1})
θ	Electrode surface bubble coverage
Δt_b	Average bubble detachment time (s)
Δt_g	Average gas film detachment time (S)
Over lined	Normalised quantities

Dedicated to Prof. Ch. Comninellis' 65th birthday.

R. El-Haddad · R. Wüthrich (✉)
Department of Mechanical and Industrial Engineering, Concordia University, Montreal, QC, Canada
e-mail: wuthrich@encs.concordia.ca

1 Introduction

As electrolysis with gas evolution is operated at high enough current densities, a continuous gas film can be formed around the working electrode. The phenomenon, often accompanied by light emission due to electrical discharges through the insulating gas layer around the electrode, is known in the literature under various names such as electrode effects, anode effects, electrochemical discharge phenomenon and contact glow discharge electrolysis. Known since more than 150 years [1, 2], several applications has emerged such as (in chronological order), reduction of metal salts [3], high frequency current interrupters [4], micro-machining of non-conductive materials [5–7], surface engineering [8], waste water treatment [9] and nano-particle synthesis [10, 11]. There are as well undesired effects related to this phenomenon such as the anode effect in the context of aluminium electrolysis [12].

Several experimental studies [13–16] of this phenomenon were conducted and theoretical models developed [17–25]. These models were essentially developed with the aim to take into account bubbles evolution for the calculation of the local current distribution in order to predict the critical current density and critical voltage at which the electrode effects appear. If the developed models considered various mechanism leading to the formation of the gas film (such as local electrolyte evaporation by Joule heating [17, 19, 20], hydrodynamic effects [18, 22], electrochemically formed gas bubbles [25]), none of them tried to incorporate the dynamics of the gas film. It is well known that the formed gas film is unstable [4, 13, 17] but it is only recently that attempts to quantify the mean life-time of the gas film, in the case of water electrolysis, were made [16]. Several applications would benefit from an increased knowledge about the dynamics of the system taking into account the gas film life-time. For example in the case of micro-machining using electrochemical discharges, the gas film dynamics is related to the quality of the machined structures [7].

The aim of the present communication is to extend our previous model [7, 25, 26] by incorporating the dynamics of the gas film with its finite life-time. A mean field version will be developed and its limitation, due to scale effects related to the gas film, will be discussed in comparison with a stochastic model.

2 Mean field model

2.1 Normalised bubble evolution equation

First a mean field model, incorporating the gas film life-time, bubble formation and detachment dynamics, is developed based on our previous one [7, 25, 26] describing the mean stationary current–voltage characteristics of a two electrode cell under high current densities. For clarity, the essential steps of the derivation of the previous model are repeated where necessary.

A two electrode set-up is considered. The gas bubble coverage on the working electrode, of surface A, is denoted as θ. From Faraday's law the amount of gas evolving on the working electrode is given by:

$$\dot{V}_g = \beta j_{local} (1-\theta) A, \tag{1}$$

with j_{local} the local current density and $\beta = \frac{nRT}{zFp}$ with the usual meaning of the used symbols. Note that the local current density should not be confused with the nominal current density $j = I/A = j_{local}(1-\theta)$ [23, 27].

In order to estimate the amount of gas bubbles leaving the electrode surface, the working electrode surface is subdivided into a lattice. Lattice sites may be occupied or empty, depending if a bubble is growing or not at that location. Neighbouring occupied sites represent larger bubbles, obtained by coalescence for example. Assuming that the mean detachment time Δt_b of a bubble is function of its size s (measured in number of sites forming the bubble), the total amount of gas leaving the electrode is given by:

$$\dot{V}_g = NAV_b \left(\sum_{s=0}^{\infty} \frac{s n_s(\theta)}{\Delta t_b(s)} + \frac{P(\theta)}{\Delta t_g} \right), \tag{2}$$

where N is the total number of sites per surface of the lattice defined on the electrode and $n_s(\theta)$ is the average number of bubbles of sizes s per lattice sites, which can be estimated using percolation theory [28]. The quantity $P(\theta)$ is the size of the infinite cluster (non zero only if $\theta > p_c$, the percolation threshold [28]) and Δt_g its mean detachment time. For simplification we will in the following assume that $\Delta t_b(s)$ depends only weakly on s and can be considered constant.

Considering 1 and 2, the mass balance equation writes:

$$\frac{d}{dt}(V_b NA\theta) = \beta j_{local}(1-\theta)A - \frac{V_b}{\Delta t_b} NA \sum_{s=0}^{\infty} s n_s(\theta) - \frac{V_b NA}{\Delta t_g} P(\theta). \tag{3}$$

Equation 3 states that gas is produced electrochemically, bubbles detach with a frequency $1/\Delta t_b$ and the gas film, if present (i.e. $\theta > p_c$), detaches with a frequency $1/\Delta t_g$. This equation can be further simplified by writing the volume of a bubble of size $s = 1$ as $V_b = \frac{h_b}{N}$, with h_b the average effective bubble height:

$$\frac{d\theta}{dt} = \frac{\beta j_{local}}{h_b}(1-\theta) - \frac{1}{\Delta t_b} \sum_{s=0}^{\infty} s n_s(\theta) - \frac{1}{\Delta t_g} P(\theta). \tag{4}$$

In the following, a dimensionless version of Eq. 4 is developed. To further simplify calculations, we assume that the inter-electrode resistance $R(\theta)$ may be estimated by:

$$R(\theta) = \frac{R^{bulk}}{1-\theta}, \tag{5}$$

with R^{bulk} the bulk inter-electrode resistance (i.e. the inter-electrode resistance without any bubble evolution).

For high enough current densities, the cell terminal voltage U is given by

$$U - U_d = R(\theta)\, I = j_{local} A (1-\theta) R(\theta), \tag{6}$$

with U_d the water decomposition potential.

From the steady-state solution of Eq. 4, together with the condition of the gas film formation ($\theta = p_c$), follows the expression for the critical voltage in accordance with the previous model [7, 26]:

$$U^{crit} = U_d + R(p_c) A \frac{h_b}{\beta\, \Delta t_b} p_c. \tag{7}$$

Combining Eqs. 4–7 yields

$$\frac{d\theta}{d\bar{t}} = \frac{p_c}{1-p_c}\bar{U}(1-\theta) - \sum_{s=0}^{\infty} s n_s(\theta) - \frac{1}{\Delta\bar{t}_g} P(\theta), \tag{8}$$

with $\bar{t} = \frac{t}{\Delta t_b}$ the normalised time and $\overline{U} = \frac{U-U_d}{U^{crit}-U_d}$ the normalised voltage. Equation 8 is the normalised bubble evolution equation of a gas evolving electrode. Note that $\Delta\bar{t}_g = \frac{\Delta t_g}{\Delta t_b}$. The quantity

$$\overline{I} = \frac{p_c}{1-p_c}\bar{U}(1-\theta), \tag{9}$$

appearing in the right hand side of Eq. 8, is termed normalised current density. In order to relate it to the measured nominal current density, one note that the nominal current density needed to form the gas film, the critical current density j^{crit}, is given by (solving Eq. 4 with the condition $\theta = p_c$):

$$j^{crit} = \frac{h_b}{\beta\, \Delta t_b} p_c. \tag{10}$$

Combining Eqs. 6, 7, 9 and 10 shows that the normalised current density is as well given by:

$$\overline{I} = p_c \cdot \frac{j}{j^{crit}} = p_c \cdot \frac{I}{I^{crit}}. \tag{11}$$

In summary, the solution of the normalised bubble evolution Eq. 8 gives the relation between the cell terminal voltage and the current density.

2.2 Gas film formation time

If a constant cell terminal voltage U is applied, the time t_f needed to build the gas film is given by the condition that $\theta(t_f) = p_c$. As for $\theta < p_c$ $P(\theta) = 0$, the gas film life-time Δt_g does not influence t_f and the new model will predict the same values as the previous one. Solving Eq. 8 for a step input $U > U^{crit}$, i.e. $\overline{U} > 1$, results in [7]:

$$\frac{t_f}{\Delta t_b} = \frac{1}{1 + \frac{p_c}{1-p_c}\overline{U}} \ln\left[\frac{\overline{U}}{(1-p_c)(\overline{U}-1)}\right]. \tag{12}$$

Equation 12 was validated experimentally in [16]. There was as well found that $\Delta t_g / \Delta t_b \approx 10-30$ with $\Delta t_b \cong 2.5$ ms. Note that Δt_g was found to increase with the cell terminal voltage. This experimental fact shows the limitation of the assumption that Δt_g is a constant.

2.3 Bistability

Figure 1 shows the stationary solution of Eq. 8 for various values of $\Delta\bar{t}_g$. The equations were solved using a Bethe Lattice with three branches. For this lattice one has [28] $p_c = 1/2$ and

$$P(\theta) = \theta + \frac{(1-\theta)^3}{\theta^2} \quad \text{if } \theta > p_c = \frac{1}{2}. \tag{13}$$

For $\Delta\bar{t}_g = 1$, i.e. the detachment time of the gas film is identical to the bubble detachment time, no gas film can be formed. For $\Delta\bar{t}_g > 1$ a gas film is formed beyond the critical point ($\bar{U}^{crit} = 1$, $\bar{j}^{crit} = p_c = 1/2$). For finite values of $\Delta\bar{t}_g$, the stationary solutions are multiple (two stable and one unstable; Fig. 2) in a defined region before $\bar{U}^{crit} = 1$. For $\Delta\bar{t}_g \to \infty$, Eq. 8 is identical to the one discussed in [25] and only one stable solution is observed. The extension of the bistable region in function of $\Delta\bar{t}_g$ is computed on Fig. 3.

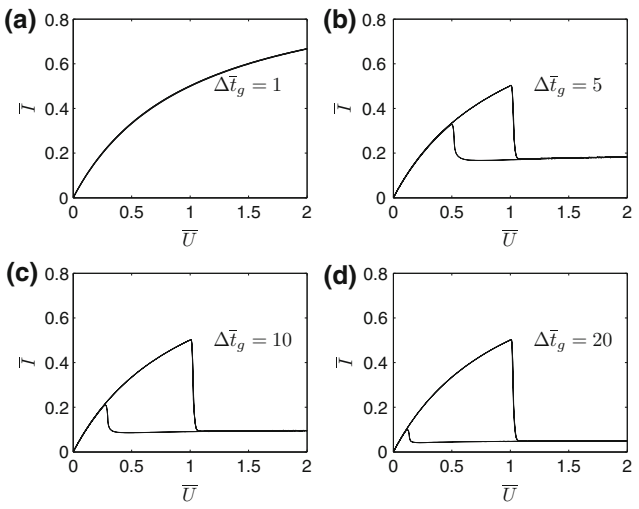

Fig. 1 Stationary solutions of the normalised bubble evolution Eq. 8 showing the dependence of the normalised current density $\overline{I}$ in function of the normalised voltage $\overline{U}$ for various gas film detachment times $\Delta\bar{t}_g$

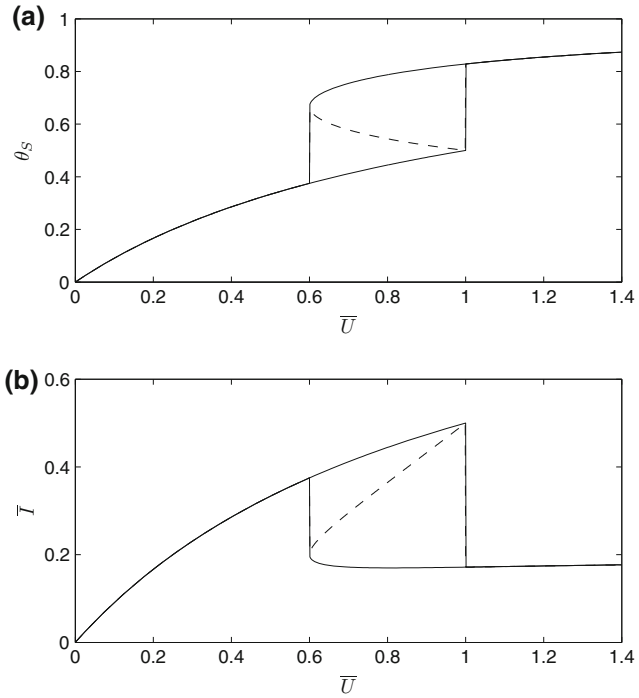

Fig. 2 **a** Stationary bubble coverage fraction θ_S as predicted by the normalised bubble evolution Eq. 8. In the interval $0.6 \leq \overline{U} \leq 1$ are two stable solutions (-) and one unstable (- -). Calculations done for $\Delta\bar{t}_g = 10$. **b** Corresponding current–voltage characteristics

Figure 4 shows non stationary solutions of Eq. 8 obtained by numerical integration using an embedded Runge–Kutta–Fehlberg algorithm [29] (combination of two Runge–Kutta methods of order four, five) with a relative error tolerance of 10^{-3}. A triangle voltage signal was applied with a scan rate $\overline{v}$ such that $\overline{U} = \overline{v} \cdot \overline{t}$ for $0 \leq \overline{t} \leq \overline{t}_f$ (forward scan) and $\overline{U} = \overline{v} \cdot \left(\overline{t}_f - \overline{t}\right)$ for $\overline{t}_f < \overline{t} \leq 2\overline{t}_f$ (reverse scan):

$$\overline{v} = \frac{\overline{U}}{\overline{t}} = \frac{U - U_d}{U^{crit} - U_d} \cdot \frac{\Delta t_b}{t}. \tag{14}$$

The normalised scan rates used were chosen in order to reproduce typical experimental conditions where scan rates are about 10 V/s. An increase in the scan rate has the effect to enlarge the bistable region (Fig. 3).

If the solutions of Eq. 8 present strong qualitative resemblances with experimental results (compare for example with Fig. 3 from [30] showing the hysteresis observed in a forward and reverse scan at 10 V/s of a two electrode cell with 30wt% NaOH), there are large quantitative discrepancies. According to [16], $\Delta t_g / \Delta t_b \approx 10-30$, which results in a bistable region extension of about 60–80% of U^{crit} (Fig. 3). However, according to [30, 31] only an extension of about 10% of U^{crit} is observed. Further, the mean current once the gas film is formed, is predicted significantly too large with this model compared to experimental observations (a few percents of j^{crit} [30, 31]). To address these issues, one has to look more closely to

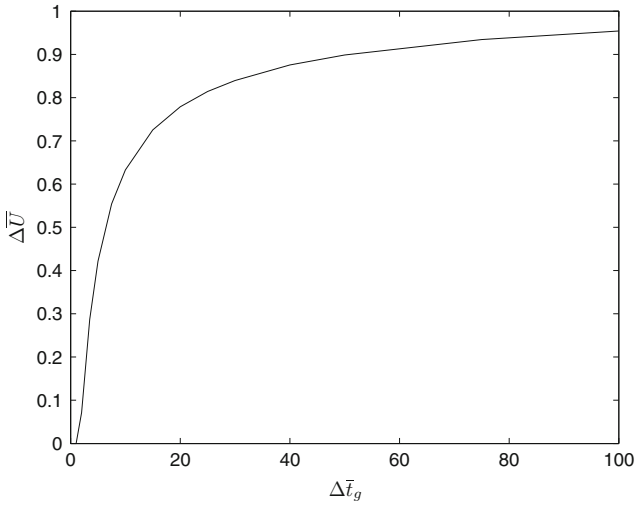

Fig. 3 Extension of the bistable region of the stationary solutions of the normalised bubble evolution Eq. 8

Eq. 8. In its mean-field version, the model assumes that in average the gas film detaches every Δt_g. However, at the moment of its detachment, the entire surface covered by the film, i.e. $P(\theta)$, becomes free of bubbles. This collective effect is not reproduced in Eq. 8. To take into account this aspect the following stochastic model is developed.

3 Stochastic model

In its stochastic version, the model assumes that the bubble evolution, as long as the gas film is not detaching from the electrode surface, is given by the following evolution equation for the bubble coverage θ:

$$\frac{d\theta}{d\bar{t}} = \frac{p_c}{1 - p_c}\bar{U}(1 - \theta) - \sum_{s=0}^{\infty} s n_s(\theta). \tag{15}$$

Further, in average every $\Delta\bar{t}_g$ the gas film detaches form the electrode surface. This is added to Eq. 15 by resetting the value of θ to $\theta - P(\theta)$ according to a Poisson process with expected value $\Delta\bar{t}_g$ if $\theta > p_c$. Figure 5 shows a typical result of a numerical simulation of this model (for $\bar{U} = 1.2$ and $\Delta\bar{t}_g = 10$; numerical integration was done using a Runge–Kutta method of order four with a Richardson error control with a relative error tolerance of 10^{-3}). The stochastic resetting of θ to $\theta - P(\theta)$ was achieved with a uniform random number distribution implemented using a linear congruential generator [29]). Note how about every $\Delta\bar{t} \approx \Delta\bar{t}_g$ a gas film is formed. The duration of the formation of a gas film is about $t_f \cong 1.2 \cdot \Delta t_b$ in accordance with Eq. 12. Note the good agreement with the experiment (compare for example with Fig. 1 from [16]).

On Fig. 6 are shown typical simulation results if a triangle voltage signal is applied with a scan rate $\overline{v}$ such that

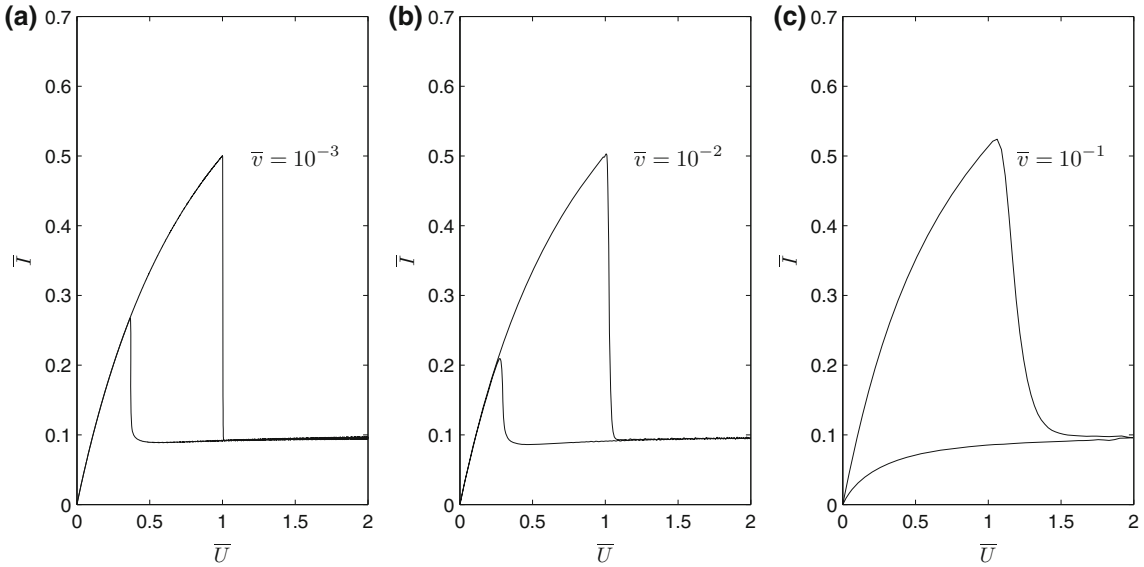

Fig. 4 Non-stationary solutions of the normalised bubble evolution Eq. 8 showing the dependence of the normalised current density $\overline{I}$ in function of the normalised voltage $\overline{U}$ for various normalised scan rates $\overline{v}$. Calculations done for $\Delta\overline{t}_g = 10$

$\overline{U} = \overline{v} \cdot \overline{t}$ for $0 \leq \overline{t} \leq \overline{t}_f$ (forward scan) and $\overline{U} = \overline{v} \cdot \left(2\overline{t}_f - \overline{t}\right)$ for $\overline{t}_f < \overline{t} \leq 2\overline{t}_f$ (reverse scan). Simulations were done over 100 scans and afterwards averaged. As in the mean field model, the forward scan is not affected by $\overline{v}$ up to the critical voltage $\overline{U} = 1$. For high scan rates, the forward scan for $\overline{U} > 1$ presents no longer an abrupt decrease but rather a smooth transition. A significant effect is seen on the reverse scan. Not only the extension of the bistable region is changed, but as well the general shape of the reverse scan. The extension of the bistable region follows

$$\Delta\bar{U} \approx \overline{v} \cdot \Delta\overline{t}_g. \tag{16}$$

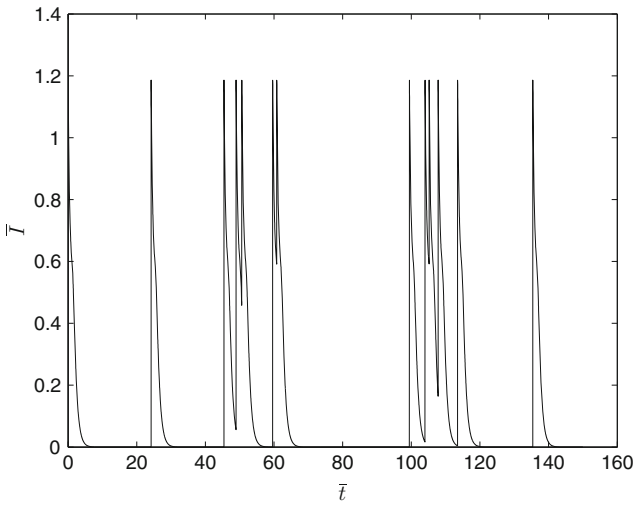

Fig. 5 Non-stationary solution of the stochastic version of the bubble evolution model. Calculations done for $\overline{U} = 1.2$ and $\Delta\overline{t}_g = 10$. The normalised current $\overline{I}$ in function of time is shown. Note how about every $\Delta\overline{t} = \Delta\overline{t}_g = 10$a gas film is detaching from the electrode surface

This can be directly seen from the stochastic model description. Indeed, during the reverse scan, once $\bar{U} < 1$ the system can no longer rebuild the gas film in case the film is lost. As the gas film is detaching in average every $\Delta\overline{t}_g$, the extension of the bistable region has to follow Eq. 16. Compared to the mean-field model, the stochastic model is in much better agreement with the experiment. The current density for cell terminal voltages larger than U^{crit} are predicted to be only a few percents of j^{crit}, which agrees well with experimental observations [30, 31]. The bistable

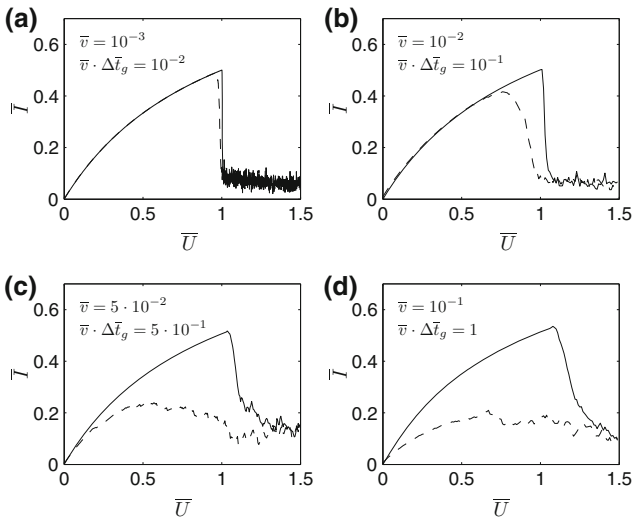

Fig. 6 Non-stationary solutions of the version of the bubble evolution model showing the dependence of the normalised current density $\overline{I}$ in function of the normalised voltage $\overline{U}$ for various normalised scan rates $\overline{v}$ in forward (-) and reverse (- -) scan. Calculations done for $\Delta\overline{t}_g = 10$; averaged over 100 simulations

region extension of about 10% of U^{crit} observed for water electrolysis at a scan rate of 10 V s^{-1} (corresponding to $\bar{v} \cdot \Delta\bar{t}_g \cong 5 \times 10^{-3}$) [30, 31] is as well much better predicted: $\Delta\bar{U} \cong 0.05$.

Equation 16 presents a great practical value. From the mean current–voltage characteristics measured in forward and reverse scan, one can directly estimate the mean gas film life-time. This is a much simpler method than the direct analysis of the time signal of the current [16] or visual observation by high speed cameras [14, 15]. Note that the knowledge of the mean bubble detachment time Δt_b is not needed for the application of Eq. 16 as this equation writes $\Delta U \approx v \cdot \Delta t_g$ in its dimensional form.

The reverse scan presents a significantly different shape than the forward scan, particularly at higher scan rates. The maximal current is smaller and presents a plateau. This plateau is observed experimentally and was so far attributed to the limitation of the gas bubbles ability to leave the electrode surface [7, 25]. The present model brings new insights into this problematic showing that, in the case of the reverse scan, this limiting current region can be due to the finite life-time of the gas film. The appearance of this plateau can be understood intuitively form the stochastic model. Recalling that the gas film detaches in average every $\Delta\bar{t}_g$ and that for $\bar{U} < 1$ it can no longer been rebuilt once lost, it becomes obvious that the average current must become smaller in the reverse than in the forward scan. The region over which this effect is noticeable will depend in the variance of the probability distribution of the gas film life-time:

$$\Delta\bar{U}^{plateau} \approx \bar{v} \cdot \mathrm{var}(\Delta\bar{t}_g). \tag{17}$$

As in the present simulations a Poisson process was chosen (i.e. the variance of the gas film life time is equal to its mean value) the extension of the plateau will follow as well Eq. 16, as can be verified on Fig. 6. A careful experimental study of the plateau of the reverse scan can therefore bring more insights about the probability distribution underlying the gas film detachment.

4 Conclusion

A model for the current–voltage characteristics of a two electrodes cell incorporating the dynamics of the gas film formed during the electrochemical discharge phenomenon is developed. In its mean-field version, the model presents good qualitative agreement with experiments but overestimates the extension of the bistable region and predicts too large current densities for cell terminal voltages higher than the critical voltage. By modifying the model in order to account for the collective detachment of the gas film, these issues can be removed. In this stochastic version of the model, the detachment as a whole is assumed to take place according to a Poisson process. Based on this model, two relations were developed which allow from the experimental study of the hysteresis in the forward and reverse scan of the two electrode cell to estimate the mean gas film detachment time and its variance.

Acknowledgments This work was supported by the Natural Sciences and Engineering Research Council of Canada (NSERC).

References

1. Fizeau H, Foucault L (1844) Ann Chim Phys XI 3ème série : 370
2. Wüthrich R, Mandin Ph (2009) Electrochim Acta 54:4031
3. Gubkin J (1887) Annal Physik 32:114
4. Wehnelt A (1899) Annal Physik 304:233. The article was originally published in 1899 Elektrotechnische Zeitschrift 4:76
5. Kurafuji H, Suda K (1968) Ann CIRP 16:415
6. Wüthrich R, Fascio V (2005) Intern J Mach Tools Manuf 45:1095
7. Wüthrich R (2009) Micromachining using electrochemical discharge phenomenon: fundamentals and applications of spark assisted chemical engraving, vol 6. William Andrew, Micro and nano technologies, Oxford
8. Yerokhin AL, Nie X, Leyland A, Matthews A, Dowey SJ (1999) Surf Coat Technol 122:73
9. Gao JZ, Wang XY, Hu ZA, Hou JG, Lu QF (2001) Plasma Sci Technol 3:765
10. Kawamura H, Moritani K, Ito Y (1998) Plasmas Ions 1:29
11. Lal A, Bleuler H, Wüthrich R (2008) Electrochem Commun 10:488
12. Vogt H, Thonstad J (2003) J Alum 79:98
13. Kellogg HH (1950) J Electrochem Soc 97:133
14. Guilpin Ch, Garbaz-Olivier J (1977) Spectrochim Acta 32B:155
15. Azumi K, Mizuno T, Akimotot T, Ohmori T (1999) J Electrochem Soc 146:3374
16. Allagui A, Wüthrich R (2009) Electrochim Acta 54:5336
17. Klupathy E (1902) Annal Physik 314:147
18. Mazza B, Pedeferri P, Re G (1978) Electrochim Acta 23:87
19. Guilpin Ch, Garbaz-Olivier J (1978) J Chim Phys Phys Chim Biol 75:723
20. Valognes JC, Bardet JP, Mergault P (1987) Spectrochim Acta 42B:445
21. Vogt H (1997) Electrochim Acta 42:2695
22. Vogt H (1999) J Appl Electrochem 29:137
23. Vogt H, Thonstad J (2002) J Appl Electrochem 32:241
24. Mandin Ph, Hamburger J, Bessou S, Picard G (2005) Electrochim Acta 51:1140
25. Wüthrich R, Comninellis Ch, Bleuler H (2005) Electrochim Acta 50:5242
26. Wüthrich R, Hof LA (2006) Intern J Machine Tools Manuf 46:828
27. Vogt H, Balzer RJ (2005) Electrochim Acta 50:2073
28. Stauffer D, Aharony A (1998) Introduction to percolation theory. Taylor and Francis, London
29. Sauer T (2006) Numerical analysis. Pearson-Addison Wesley
30. Wüthrich R, Baranova EA, Bleuler H, Comninellis Ch (2004) Electrochem Commun 6:1199
31. Wüthrich R, Hof LA, Lal A, Fujisaki K, Bleuler H, Mandin Ph, Picard G (2005) J Micromech Microeng 15:268